Supplemental material

Malhotra et al., https://doi.org/10.1084/jem.20172021

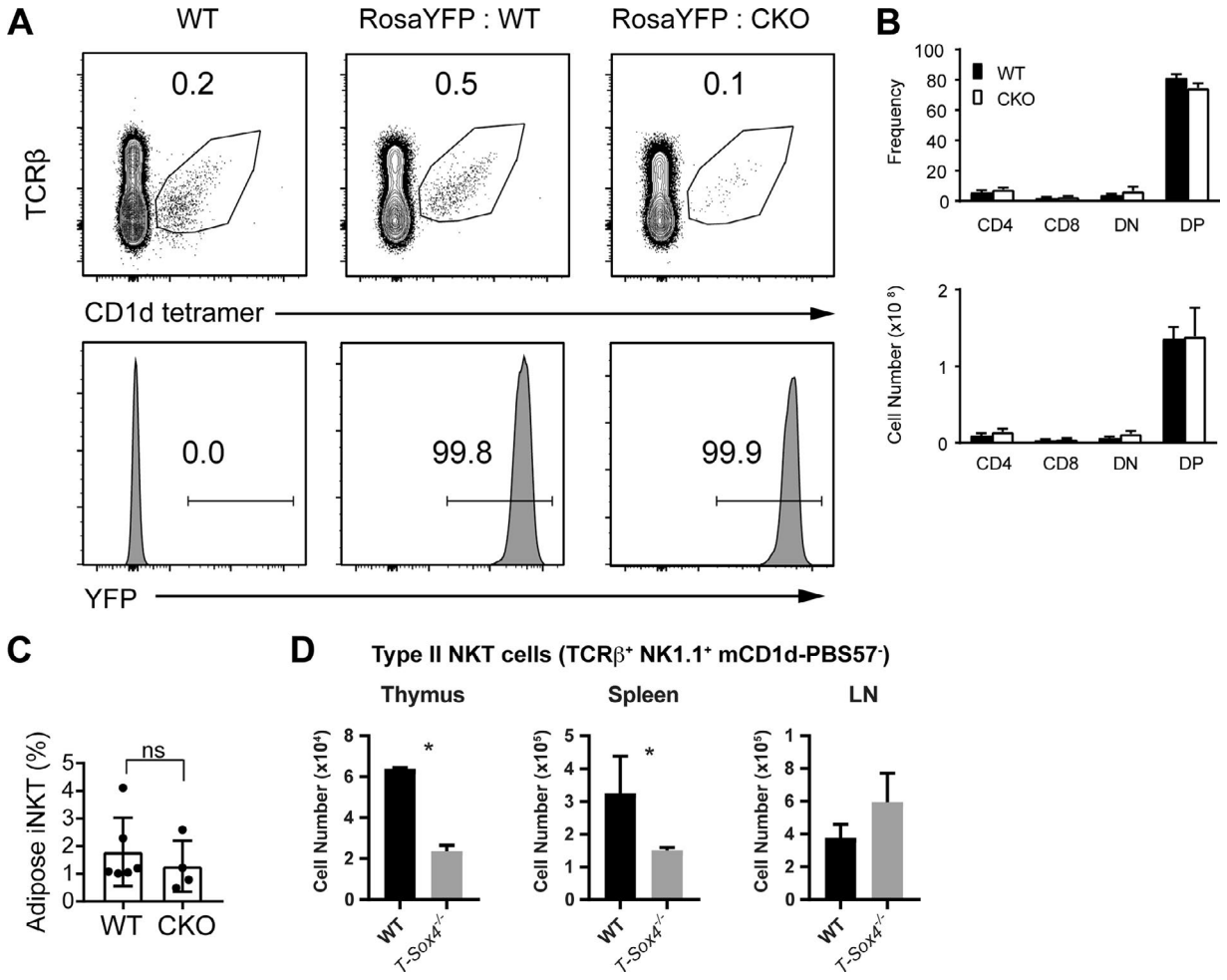

Figure S1. **Characterization of T-*Sox4*$^{-/-}$ mice. (A)** Complete deletion of "floxed" *Sox4* gene using *Cd2*-iCre driver. *Cd2*-iCre:*Sox4*$^{fl/fl}$; ROSA-Stop$^{fl/fl}$-*Yfp* (RosaYFP:CKO) and control *Cd2*-iCre:*Sox4*$^{+/+}$; ROSA-Stop$^{fl/fl}$-*Yfp* (RosaYFP:WT) mice were generated to determine the extent of *Sox4* deletion in iNKT cells. Histograms show the frequencies of YFP$^+$ cells (indicative of Cre activity and a proxy for the frequency of cells with excised *Sox4*) among total iNKT cells in nonlittermate reporter-negative control C57BL/6 (WT), littermate RosaYFP:WT versus RosaYFP:CKO mice. n = 4/genotype, except WT, n = 2. **(B)** Frequencies and numbers of conventional αβ T cell developmental intermediates in the thymus of WT (Cre$^+$) and CKO littermates, indicating normal subset distribution in the absence of *Sox4*. n = 7/genotype. **(C)** Frequencies of iNKT cells in the adipose tissue of WT and CKO mice. Each dot represents an individual mouse. Numbers of hematopoietic cells isolated were variable from mouse to mouse, but there was no difference in average numbers in WT and CKO mice. Statistics based on Student's t test. **(D)** Summary of type 2 NKT cell numbers in thymus, spleen, and peripheral LN of WT and T-*Sox4*$^{-/-}$ CKO mice. Data are from one of three similar experiments with n = 5–6 per genotype. *, P < 0.05 by unpaired t test. Error bars denote SD.

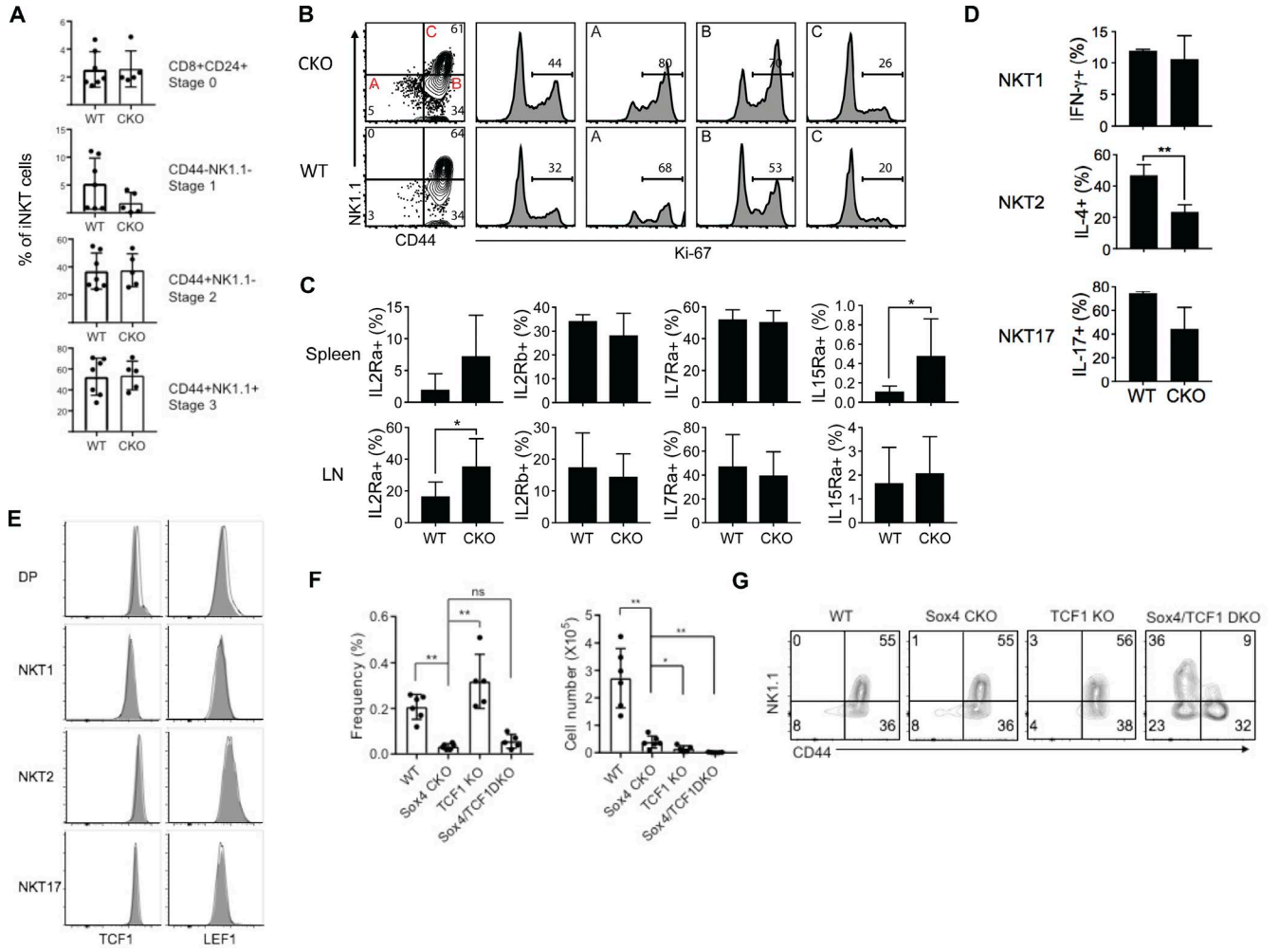

Figure S2. **Proliferative status of *Sox4*-deficient thymic iNKT cell developmental intermediates and iNKT phenotype of *Sox4-Tcf7* compound mutants. (A)** Proportions of iNKT developmental intermediates based on CD8, CD24, CD44, and NK1.1 expression in ∼6-wk-old WT and CKO mice are shown. Total thymic cellularity of CKO mice overlaps with that of WT mice at this age, and the relative difference in frequencies indicates numerical difference. Each dot represents an individual mouse. One of five independent experiments. **(B)** Frequencies of thymic iNKT developmental intermediates in active cell cycle, as detected with Abs specific for Ki-67. Stage 1 (A), Stage 2 (B), and Stage 3 (C) iNKT cells are shown, with Ki-67 expression in total iNKT cells (no letter gate) shown as a reference. Representative profiles from one of four independent experiments. **(C)** Analysis of cytokine receptor expression on total iNKT cells from spleen or LN of WT and CKO mice. Data are pooled from two independent experiments with $n = 5–6$/genotype. *, $P < 0.05$ by unpaired t test. **(D)** Effector cytokine production from residual iNKT cells of *Sox4*-deficient mice. Thymic iNKT cells were stimulated with PMA and Ionomycin and then analyzed for both TFs and intracellular cytokines. Cells were gated on live, B220/CD19$^-$ TCRβ$^+$ mCD1d-PBS57$^+$, and then NKT1 = T-bet$^+$RORγt$^-$, NKT2 = CD24$^-$NK1.1$^-$ (Stage 1/2; in our hands, IL-4 staining did not give consistent results in buffers used for TF staining), and NKT17 = RORγt$^+$T-bet$^-$. Data are summarized from three independent assays. **(E)** No alterations in TCF1 and LEF1 expression in *Sox4*-deficient iNKT cells. Profiles of intracellular/intranuclear TCF1 and LEF1 expression in DP, NKT1 (T-bet$^+$), NKT2 (PLZF^{hi}), and NKT17 (RORγt$^+$) subsets. Thymocytes from WT and CKO mice are depicted in shaded gray and black line, respectively. Representative of two independent experiments. **(F)** Most severe reduction in iNKT cells is observed in *Tcf7*$^{-/-}$*Sox4* CKO double KO (DKO) mice. Statistical significance based on Student's t test (*, $P < 0.05$; **, $P < 0.01$; ns, not significant). Frequencies and cell numbers of total thymic iNKT cells from WT, *Sox4* CKO, *Tcf7*$^{-/-}$ (KO), and DKO mice. Each dot represents an individual mouse (∼6 wk old). Data are from three independent experiments. Error bars denote SD. **(G)** Representative flow cytometric profiles of thymic iNKT cell developmental intermediates in the indicated strains. Representative data from three independent experiments.

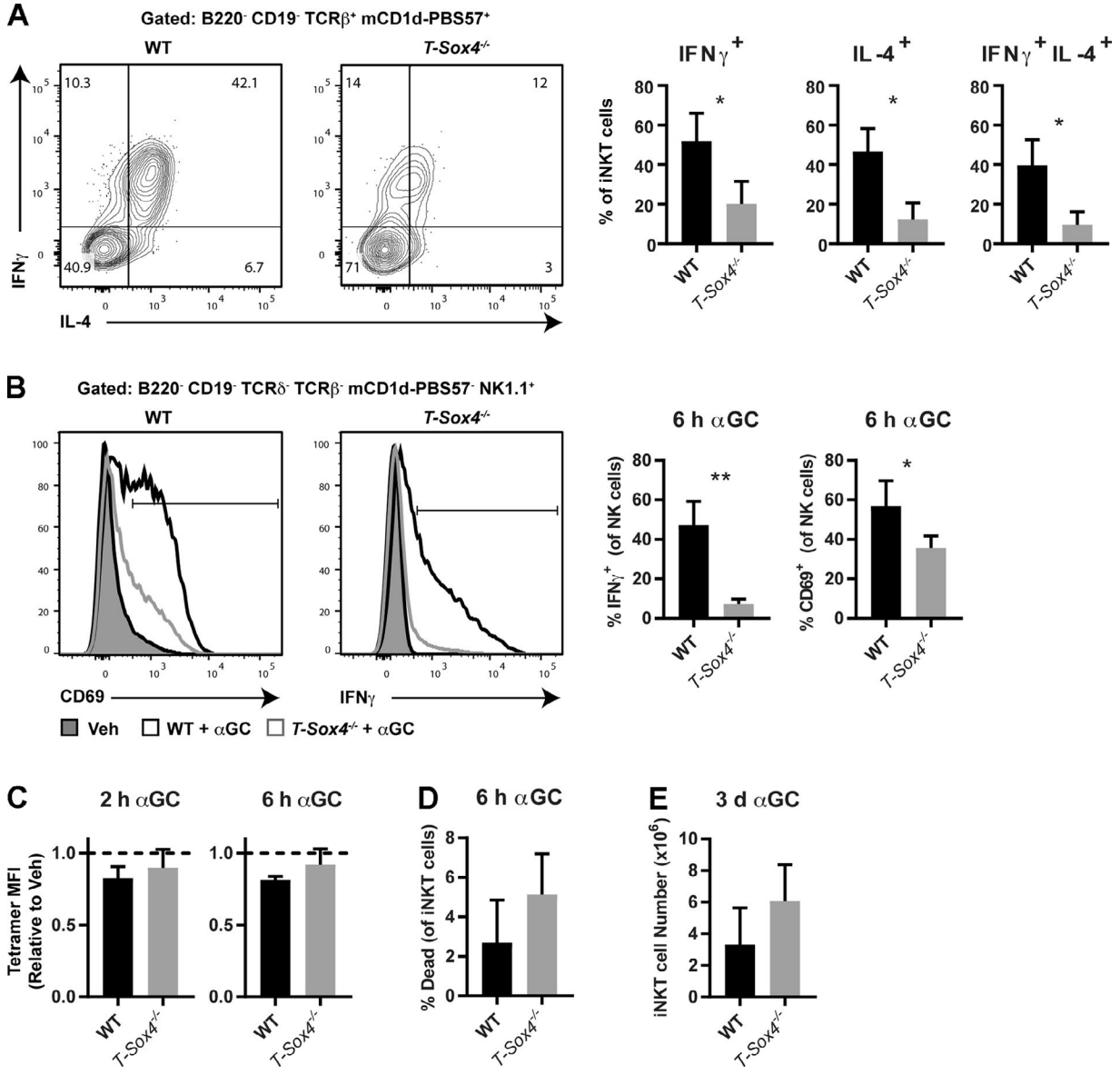

Figure S3. **Responses to in vivo αGC administration in T-*Sox4*$^{-/-}$ mice.** For all experiments, mice were injected intravenously with 2 µg αGC or vehicle (Veh, 1% DMSO in PBS) only control. **(A)** iNKT cell cytokine production was examined 2 h after αGC injection. Gates are based on cytokine staining of iNKT cells from Veh-injected mice. For the IFNγ$^+$ plot, this includes all IFNγ$^+$ cells (i.e., IL-4$^+$ and IL-4$^-$); for the IL-4$^+$ plot, this includes all IL-4$^+$ cells (i.e., IFNγ$^+$ and IFNγ$^-$). *n* = 3/genotype. *, P < 0.05 by unpaired *t* test. **(B)** Transactivation of NK cells was assessed by CD69 and IFNγ staining 6 h after αGC injection. CD69$^+$ gate is based on FMO control, and IFNγ$^+$ gate is based on Veh-injected mice. *n* = 3/genotype. *, P < 0.05; **, P < 0.01 by unpaired *t* test. **(C)** TCR down-modulation was examined by comparing the mCD1d-PBS57-tetramer median fluorescence intensity (MFI) of iNKT cells from αGC-injected mice to that of iNKT cells from Veh-injected mice at 2 or 6 h after injection. *n* = 3/genotype and time point. **(D)** iNKT cell death was assessed 6 h after αGC injection by analyzing the frequency of cells positive for the fixable viability dye. *n* = 3/genotype. **(E)** iNKT cell numbers were calculated 3 d after αGC injection of WT and T-*Sox4*$^{-/-}$ mice. *n* = 3/genotype. Error bars denote SD.

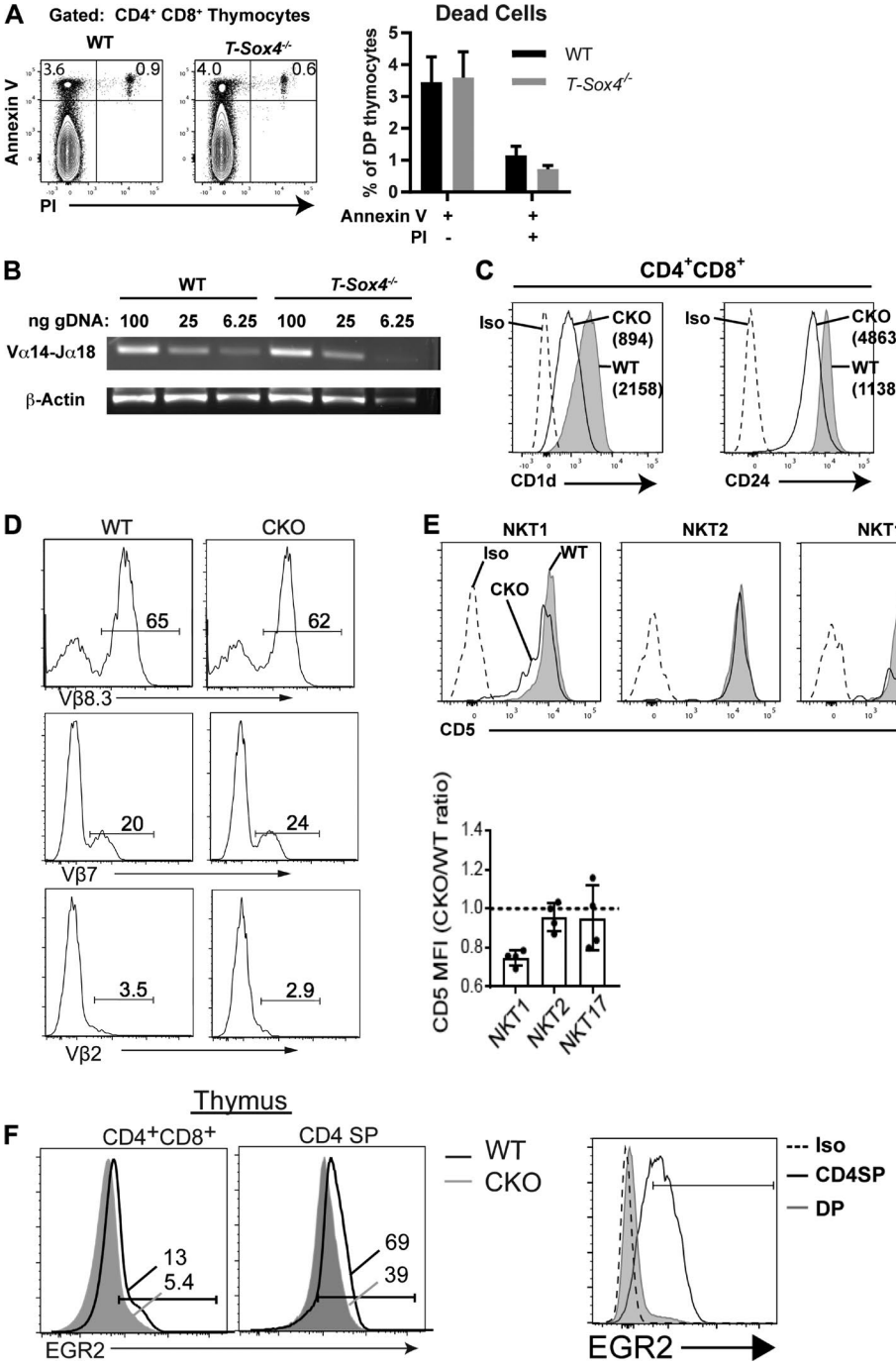

Figure S4. **SOX4-dependent alterations in molecules that impact intrathymic TCR signaling in developing iNKT cells. (A)** Assessment of DP thymocyte survival in WT and T-*Sox4*$^{-/-}$ mice by Annexin V and PI staining. Data are from five to six mice/genotype from two independent experiments. **(B)** DP thymocytes were sorted from WT and T-*Sox4*$^{-/-}$ mice for isolation of genomic DNA (gDNA) and subsequent assessment of Vα14-Jα18 TCR rearrangement. β-Actin amplification was used as a control. Data are representative of three independently sorted samples. **(C)** Decreased expression of CD1d and CD24 on *Sox4*-deficient DP cells. Histograms show relative CD1d and CD24 expression on DP cells as indicated by MFI. Representative profiles from three (CD1d) and five (CD24) independent experiments. WT, filled gray curve; CKO, black line; isotype control Ab (Iso), black dashed line. Note that all DP cells express these two surface molecules, and no DP cells from CKO mice completely lack expression of either molecule. **(D)** TCRVβ chain usage in *Sox4*-deficient thymic iNKT cells is not different from WT comparators, as determined by flow cytometric analyses of the three primary Vβ chains expressed by iNKT cells. Same results in LN iNKT cells are not shown. One of three independent experiments. **(E)** Decreased CD5 expression in *Sox4*-deficient thymic NKT1 cells. Top, Histograms show CD5 expression on indicated thymic NKT subsets. WT, filled gray curve; CKO, black line; isotype control Ab (Iso), black dashed line. Representative profiles from three independent experiments. Bottom, CKO/WT ratios of CD5 MFI of thymic iNKT subsets. *n* = 4/genotype. **(F)** Decreased EGR2 expression in CKO thymic subsets. Intracellular/intranuclear EGR2 expression in DP and CD4$^+$ SP thymocytes of WT (CD-2iCre$^+$) and CKO mice. Numbers represent proportions of EGR2$^+$ cells as gated. WT, black line; CKO, filled gray curve. Representative profiles from two experiments. The array data indicated significant differences at the transcript level that barely missed the arbitrary twofold change cutoff and is not noted on Fig. 4 A. Right, isotype and biological controls for the EGR2 Ab staining performed independently is also shown. Error bars denote SD.

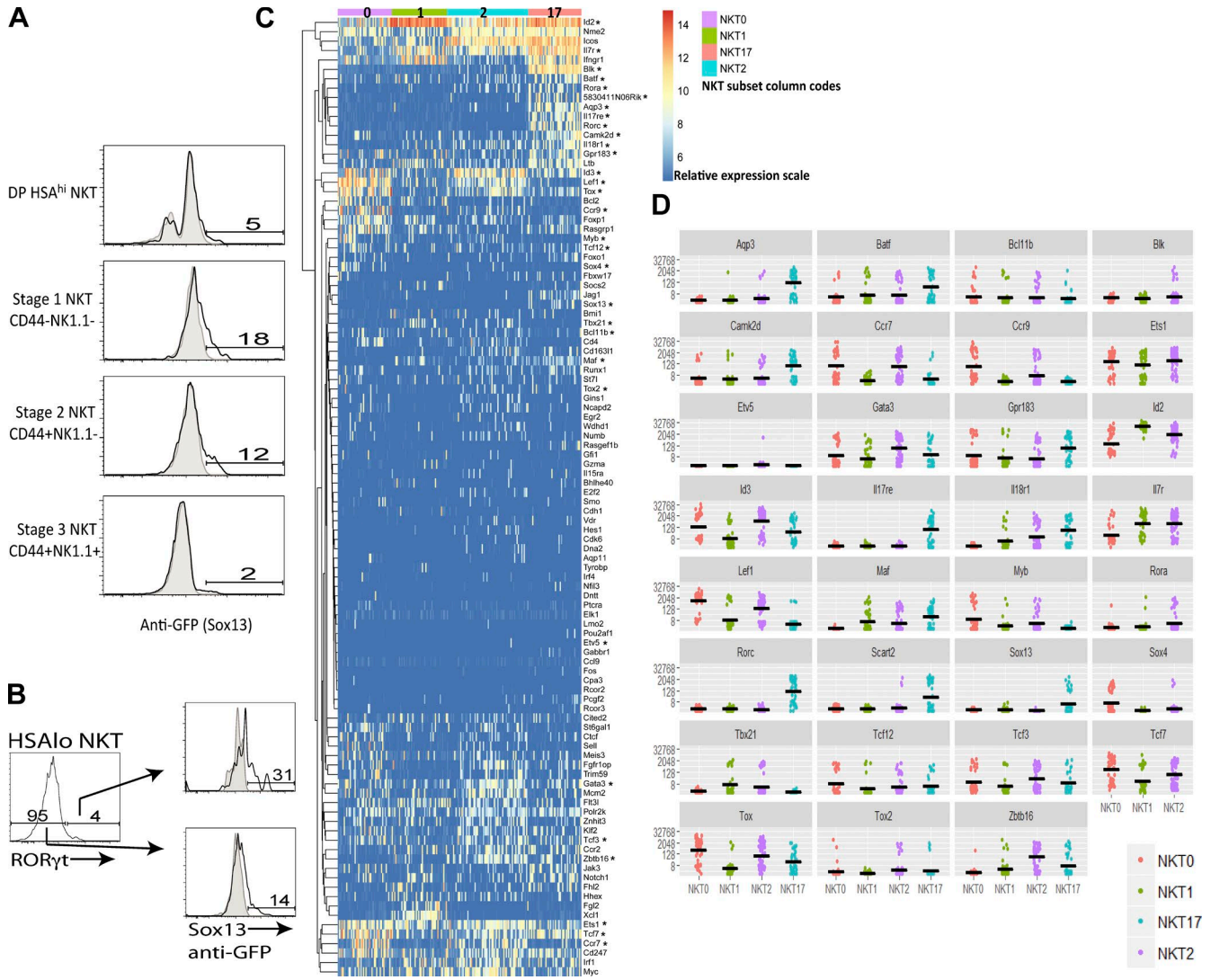

Figure S5. **Expression of *Sox13* and the Tγδ17 gene signature in iNKT cells. (A)** Intracellular staining of ECFP reporter shows evidence for *Sox13* promoter activity in Stage 1 and 2 iNKT cells. Note that icECFP does not necessarily correlate with active endogenous *Sox13* transcription, as icECFP can be retained in cells upon cessation of transcription and only lost after subsequent cell divisions. One of two experiments shown. Anti-GFP Ab cross-reacts with all GFP derivatives, including ECFP. **(B)** Higher expression of icECFP in RORγt^{+} iNKT cells (top right) compared with RORγt^{neg} iNKT cells (bottom right). **(C)** Heat map depicting relative expression levels (color code on the right) of 102 genes used to discriminate the Tγδ17 gene signature in thymic iNKT subset (denoted at the top and color code on the right) single-cell RNaseq dataset (GSE74597) from the Kronenberg laboratory (Engel et al., 2016). The gene list is based on Narayan et al. (2012) and Spidale et al. (2018), and expression spectra of the genes in single thymocytes (precursors and γδTCR^{+} thymocytes) were confirmed using the Fluidigm single-cell gene expression analysis and/or the Chromium single-cell solution from 10X Genomics (Immunological Genome Project Consortium, 2018; unpublished data). **(D)** Dot plot representations of the dataset in C, focused on the core Tγδ17 gene signature consisting of 31 genes, including *Sox13*. These genes are marked with an asterisk (*) on the heat map in C for cross-references. Each dot represents normalized expression values (left) from one cell, and each column represents an iNKT subset, as denoted (bottom right).

References

Engel, I., G. Seumois, L. Chavez, D. Samaniego-Castruita, B. White, A. Chawla, D. Mock, P. Vijayanand, and M. Kronenberg. 2016. Innate-like functions of natural killer T cell subsets result from highly divergent gene programs. *Nat. Immunol.* 17:728–739. https://doi.org/10.1038/ni.3437

Immunological Genome Project Consortium. 2018. Immunological Genome Project. Available at: immgen.org (accessed September 1, 2018).

Narayan, K., K.E. Sylvia, N. Malhotra, C.C. Yin, G. Martens, T. Vallerskog, H. Kornfeld, N. Xiong, N.R. Cohen, M.B. Brenner, et al. Immunological Genome Project Consortium. 2012. Intrathymic programming of effector fates in three molecularly distinct γδ T cell subtypes. *Nat. Immunol.* 13:511–518. https://doi.org/10.1038/ni.2247

Spidale, N.A., K. Sylvia, K. Narayan, B. Miu, M. Frascoli, H.J. Melichar, W. Zhihao, J. Kisielow, A. Palin, T. Serwold, et al. 2018. Interleukin-17 producing γδ T cells originate from SOX13+ progenitors that are independent of γδTCR signaling. *Immunity.* In press.